applied sciences

MDPI

Article

The Design of a Smart Lower-Limb Prosthesis Supporting People with Transtibial Amputation—A Data Acquisition System

Cristina Floriana Pană [1], Liviu Florin Manta [1,*], Ionel Cristian Vladu [2,*], Ștefan Irinel Cismaru [1], Florina Luminița Petcu (Besnea) [1], Dorian Cojocaru [1] and Nicu Bîzdoacă [1]

[1] Department of Mechatronics and Robotics, University of Craiova, RO-200440 Craiova, Romania; cristina.pana@edu.ucv.ro (C.F.P.); stefan.cismaru@edu.ucv.ro (Ș.I.C.); florina.petcu@edu.ucv.ro (F.L.P.); dorian.cojocaru@edu.ucv.ro (D.C.); nicu.bizdoaca@edu.ucv.ro (N.B.)

[2] Department of Electromechanical, Environmentaland Computer Science Applied in the Electrical Engineering, University of Craiova, RO-200440 Craiova, Romania

* Correspondence: florin.manta@edu.ucv.ro (L.F.M.); cristian.vladu@edu.ucv.ro (I.C.V.); Tel.: +40-740-292334 (L.F.M.); +40-728-148258 (I.C.V.)

Abstract: For people with amputated lower limbs, it is imperative to make high-performance prostheses that reproduce, as accurately as possible, the functions of the amputated limb. In this case, a preliminary study of the lower limbs from a kinematic and dynamic point of view is necessary. This paper proposes a prosthesis design and a system for acquiring the information needed to determine the stepping phase kinematic and dynamic parameters of the legs. This system consists of a sensory system attached to the legs and a acquisition data unit built around a microcontroller. The sensory system is based on a sensory system for determining the weight distribution on the sole, made of resistive pressure sensors. The sensory system will be subjected to measurement repeatability and homogeneity tests to evaluate and validate the accuracy and error of the proposed solution. The data obtained by the sensory system is transmitted in real-time, via wi-fi, to a computer system for interpretation. After processing and interpreting the data using standard data sets for comparison, the position of the legs, the type of gait and the phase of movement can be determined. Constructively, the system is configurable and can be adapted to any person, male or female, regardless of shoe size.

Keywords: prosthesis; resistive pressure sensors; acquisition system

check for updates

Citation: Pană, C.F.; Manta, L.F.; Vladu, I.C.; Cismaru, Ș.I.; Petcu (Besnea), F.L.; Cojocaru, D.; Bîzdoacă, N. The Design of a Smart Lower-Limb Prosthesis Supporting People with Transtibial Amputation—A Data Acquisition System. *Appl. Sci.* **2022**, *12*, 6722. https://doi.org/10.3390/app12136722

Academic Editors: Ionuț Daniel Geonea and Cristian Copilusi Petre

Received: 18 March 2022
Accepted: 28 June 2022
Published: 2 July 2022

Publisher's Note: MDPI stays neutral with regard to jurisdictional claims in published maps and institutional affiliations.

Copyright: © 2022 by the authors. Licensee MDPI, Basel, Switzerland. This article is an open access article distributed under the terms and conditions of the Creative Commons Attribution (CC BY) license (https://creativecommons.org/licenses/by/4.0/).

1. Introduction

Amputation of the limb or extremity of a limb, either from the upper extremity amputation (UEA) or lower extremity amputation (LEA) of the human body, affects people's quality of life. Globally in 2017, the highest number of trauma amputations was in East and South Asia, followed by Western Europe, North Africa and the Middle East, increasing in North America and Eastern Europe [1].

In a 28-year study (1990–2017) on the incidence of lower extremity amputations in 19 countries (EU15+) by Hughes et al. [2], significant geographic and temporal variability was observed. According to this study, Australia had the highest incidence of LEA in women and men during the study period. However, this incidence decreased steadily in the Netherlands and the USA, and a higher percentage reduction is found in the USA. Another recent study examined Germany's LEA incidence from 2015 to 2019 [3]. According to this study, in 2019, compared to 2015, the incidence of major amputations decreased by 7.3%, while the incidence of minor amputations increased by 11.8%, and there was also a decrease in the incidence of women to men.

In terms of the causes that led to the amputation of the lower limbs, demographically, there are many differences between developed and developing countries. For example,

compared to developed countries where most amputations are due to disease processes such as diabetes, the causes of amputations are more related to environmental factors, living conditions, or wars in developing countries [4].

Individuals who have had lower limb amputations face many other physical challenges that can compromise their health and mobility. Hence the need for a technical replacement (prosthesis) that restores the biomechanical function of the amputated element and the body's integrity. Management of lower limb prostheses for these individuals is a complicated issue. Unfortunately, the candidates who want to benefit from the usefulness of a prosthesis are a heterogeneous group with distinct ages and needs. In addition, the choice of the perfect candidate depends on the following factors: the aetiology of limb loss, the level of amputation, comorbidities and health, the postoperative stage, and the state of rehabilitation. Lower limb prostheses can be classified into three types of devices: passive, semi-powered or powered. For example, individuals with transtibial amputation (the term transtibial indicates that the amputation occurred between the knee and the ankle) are usually prescribed a prosthesis for storage and return of passive elastic energy, made of carbon fibre and works as an arc without the ability to generate energy again or to articulate. Most ankle and foot prostheses available on the market until the early 2000s were completely passive. The simplest solution for transtibial amputations is a solid prosthesis of the foot without an ankle joint [5]. As a result, the mechanical properties did not adapt to the user's walking speed and terrain type. Individuals with transtibial amputation often adopt compensatory gait strategies. These can lead to significant changes in gait dynamics, the joints loading and working, and the muscular activity of the affected and unaffected leg [6]. In the last three decades, approaches in prosthetic technology have led to significant advances, especially regarding biomechanical and user comfort [7] and in walking symmetry and energy cost [8]. An excellent example of a marketable passive prosthetic foot is the C-Walk [9], equipped only with passive components but combined suitably. As a result, it is more effective from an energy point of view compared to other prostheses in this category.

The first electrically powered ankle-foot prosthesis was built in 1998 and was pneumatically operated [10]. Subsequently, from 2005 until now, studies have focused on designing and developing autonomous energy supply systems [11–18]. The main factors considered for the design of prostheses are both the mechanical properties [19,20] and the length of the prosthesis [21]. Another factor that should not be overlooked is the weight of the prosthetic components [22]. A higher weight also increases the stress on the socket—the residual connection of the limbs, which is one of the most critical elements in the prosthesis [23]. In addition, most studies in the literature have been conducted on the evaluation of kinematic and kinetic gait [24] and foot plantar pressure [25,26].

Magnetorheological fluids (MR) were successfully introduced into prosthetic devices after 2000. In 2001, a patent was published [27] for a variable torque magnetorheological knee prosthesis produced by Ossur Inc, Los Angeles, CA, USA [28]. Herr and Wilkenfeld [29], in 2003, presented a magnetorheological knee prosthesis that automatically adjusts the cushioning of the knee to walking amputated using only local detection of the knee, torque and strength position. In 2006, a study related to [27] was carried out, which was intended to be part of a project to create models with finite elements of the knee [30]. Another invention patent [31] was published in 2012 generally relating to powered human augmentation devices, such as lower-extremity prosthetic, orthotic, or exoskeleton apparatus, and/or humanoid robotic devices designed to emulate human biomechanics. Among the most current studies is [32], which analyzes the energy consumption of a magnetorheological active knee actuator that has been designed for transfemoral prostheses. The system was developed as an operational motor unit consisting of an EC motor, a harmonic drive, and a magnetorheological clutch (MR) parallel with an MR brake.

By analyzing the above literature, it can be said that significant advances have been made in the research and development of prostheses for the lower limbs, which has led to an increase in the function and quality of life for many people with amputations of the lower

limbs living in developed countries. However, one downside of this new research and development is that many potential users live in developing countries and cannot benefit from this new technology. This fact is due to multiple causes: cost, durability, maintenance or access to these prostheses. Under these conditions, research needs to focus on designing and developing cost-effective foot prostheses that meet economic, environmental and physical standards to cope with unfavourable climates and working conditions. So far, many cheap prosthesis projects have been done to support the lower limbs, such as [33–35]. Our team aims to design and implement a low-cost prosthesis to support people with lower limb amputation (especially transtibial amputation). In the first phase, two goals were set: to design the smart ankle prosthesis and implement a solution to determine the weight distribution on the sole. The smart ankle prosthesis is intended to be developed as a passive one (from the articulation actuation point of view) and controllable (by using a magnetorheological fluid and controlling its properties to obtain a controllable damping effect inside the articulation). For the weight distribution on the sole, in this stage of our research, we will propose an alone sandal with eight pressure sensors. The first objective we set for the current study is to propose a smart ankle prosthesis design; the second objective is to design, develop, and validate a solution to determine the weight distribution on the sole; the third objective is to conduct a series of measurements which allow us to test the data acquisition system firstly and to compare the acquired data against other systems presented in the literature, and secondly to create a dataset which will be used to design a future algorithm which to detect the gait phases. With these parameters determined, it is possible to control the optimal position of the prosthesis joints, depending on the phase and the type of movement. The determinations were made for people without amputated limbs. The appropriate values for an amputated limb can be determined by mediating their values. This simplified and optimized system can be integrated into a prosthesis for its configuration in real-time, regardless of the phase or type of movement.

Our Prosthesis Design

The research effort in this field focuses on improving the characteristics of the artificial ankle to closely simulate the human ankle's functionality. The design of an artificial ankle involves many scientific and technical areas such as medicine, robotics and mechatronics, biomechanics, material science, mechanical engineering, electronics, and others. The challenge of the ankle prosthesis design is to find the means to achieve the functions of an intact ankle, especially the role of power generation.

This study presents an innovative solution for a smart ankle prosthesis based on smart fluids that will simulate the functionality of the human ankle for both walking and running activities.

The mechanical structure consists of the mechanical elements of a standard prosthesis (Figure 1). The innovative element will be a spherical joint based on smart fluids (class 4), which replaces the human ankle joint. The spherical joint allows two rotations, corresponding to the up and down movement and the lateral rotation of the foot. For each rotation, the spherical joint consists of two concentric hemispherical shells between which there is a magnetorheological fluid. The volume between the two spherical shells is divided in two by a fixed belt. Also, a spherical cap rotates between the two spheres. It is rigidly attached to the prosthesis elements, rotating with them and generating the rotational movement of the ankle. Angle 0 divides the fluid into two equal volumes for the relaxation position.

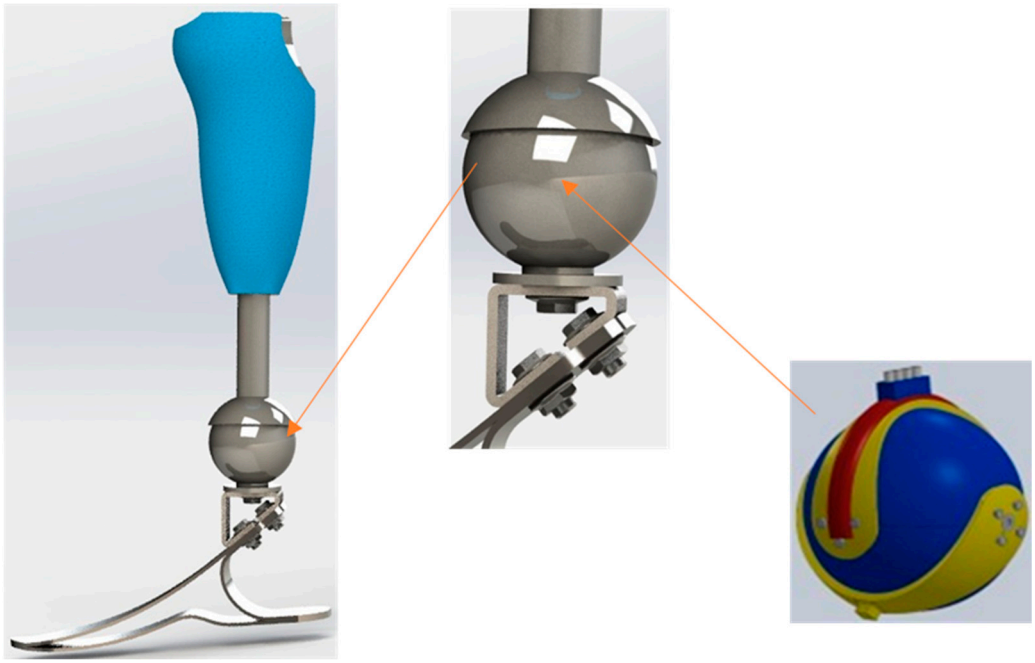


Figure 1. Ankle prosthesis with smart fluid joint.

At the rotation between the two hemispheres, the fluid is circulated from one space to another through a magnetorheological stop valve (outside the joint). Due to the incompressibility of the fluid through the control of the stop valve, the control of the rotation of the spherical cap between the two hemispheres is obtained, so implicitly, the control of the rotation of the joint. For the second axis of rotation, proceed similarly. The joint is shown in Figure 2. Its detailed description is presented in the works [36]. Also, the mechanical system contains the reconstruction of the leg components that have been amputated (ankle, leg, etc.).

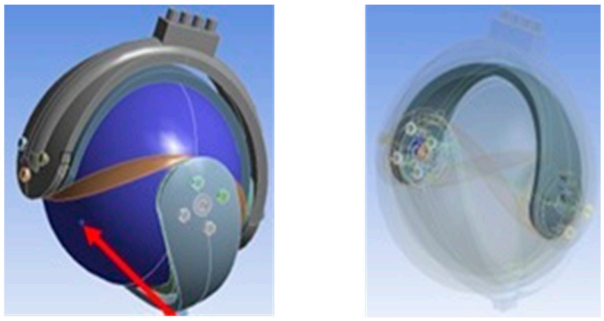


Figure 2. Spherical joint based on smart fluids (magnetorheological fluid).

The actuator system: The prosthesis uses elastic elements that maintain the foot's position in the relaxation position. Also, the ankle joint allows rotation (lateral and vertical) under the action of body weight (support on foot, walking, running). A stop-valve controls both movements of the joint with rheological fluid. After the cessation of the effort (due to the move), the elastic elements bring the paw to the position of relaxation.

The sensorial system: The sensory system provides information about the position of the articulation of the prosthesis and the force exerted on it due to the body's movement (size, direction). The information is provided to the control system. It consists of incremental rotation sensors (associated with the spherical joint) and force sensors (associated with the foot paw). In addition, the value of the working pressures for the stop valve is given by pressure sensors.

The control system: Prosthesis control systems must accomplish multiple tasks, such as recognizing the amputee's intended movements (high-level control), applying an appropriate control law based on the amputee's intent (mid-level control), and using local feedback to command the actuation systems within the prosthesis (low-level control). The control system will be capable of controlling the ankle joint across various ambulation modes (level-ground walking, ramp ascent/descent, stair ascent/descent, running); however, these control strategies are highly sophisticated.

There is a known ankle prosthesis that solves this problem through two constructive solutions, namely:

(1) The most used solution is the prosthetics leg for normal daily activities (upright position, walking, etc.). Generally, they are designed strictly for one person (weight, dimensional) and a spherical joint of class 5 that allows vertical movements of the foot. Most of these prostheses are passive, and the movement control is performed (strictly mechanical) by elastic elements or hydraulic/pneumatic cylinders. These have the disadvantage of the need for design strictly reported to a beneficiary. They also allow only one type of activity (e.g., walking) [37].
(2) Another solution is the prosthetic for particular activities (sports activities: running, jumping). They are generally built from a single elastic body without containing the rotating joint. Therefore, they are dedicated only to sports activities, designed only for certain types of requests, strictly for one person. To switch to daily activities, it is necessary for this person to change the prosthesis [38].

The classical spherical joints do not control the movement of interconnected elements, having only the role of a passive kinematic couple.

Our spherical joint based on smart fluids was proposed in a national patent application: Spherical joint based on intelligent fluids—A/00213/2019 [39] and was a gold medalist at Euro Invent 2019.

The rest of the paper is structured as follows: Section 2 presents the design of the prosthesis and the sensory system, as well as the data validation of the sensory system; Section 3 shows the results obtained from the simulations; Section 4 presents the challenges associated with the development of such systems and their potential solutions, as well as a discussion about the future research perspectives are given; finally, Section 5 is devoted to the conclusions.

2. Materials and Methods

2.1. Acquisition System for Determining the Phase of Passing and Walking Characteristics

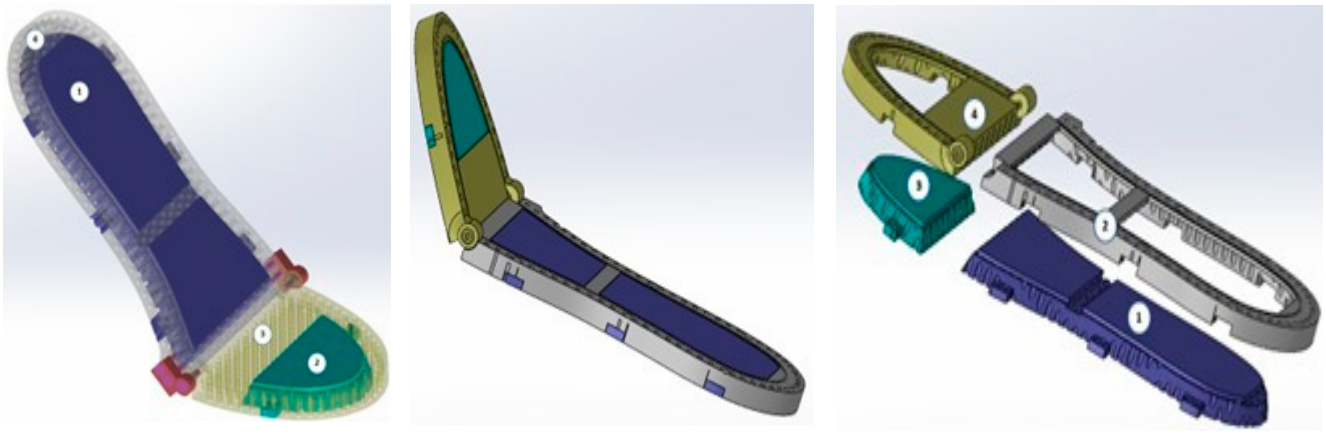
The proposed sensorial system includes force sensors, which to provide a reliable plantar pressure measurement.

Plantar pressure measurement systems, including low-cost insole sensors, are trendy instruments used in diagnosing foot disorders [40] and for monitoring the rehabilitation process. We consider that the plantar pressure measurement can be used as an input for our active prosthesis control system. Currently, there are many commercial systems with a high density/large number of pressure sensors, having a limited charging time. From a transtibial active prosthesis control point of view, there is not a need for such a high density of plantar pressure measurement points. Also, the above-mentioned commercial solutions are designed to help determine the mode of complex information, i.e., the deviations of the spine and determinations made at rest. They are rigid systems of the type of pressure plates or flexible for the kind of insoles with insertion of pressure elements. Neither of the two systems satisfies the objective proposed in the paper—to provide reliable data about the plantar pressure to be used by the control system. There is also no integrated system that simultaneously reads the sole load and the kinematics or dynamics of the foot. Therefore, the first objective of the authors of this paper was to develop a low-cost insole prototype composed of an adequate, small number of sensors, which offer the optimum data about the plantar pressure.

A special shoe, like a sandal, with a rigid sole, was made for this. On its sole are mounted eight resistive pressure sensors in the three areas of interest. In addition, the foot straps are mounted on the top. The sandal is made modularly and, with minimal modifications, can be adapted to any size of shoes 36–41 women and 41–46 men. This implies the design of a highly customizable sandal sole, the manufacture of it using a 3D printer/ABS filament, identifying the optimal placement for the sensorial units, and the design and manufacture of an accurate and reliable data acquisition system.

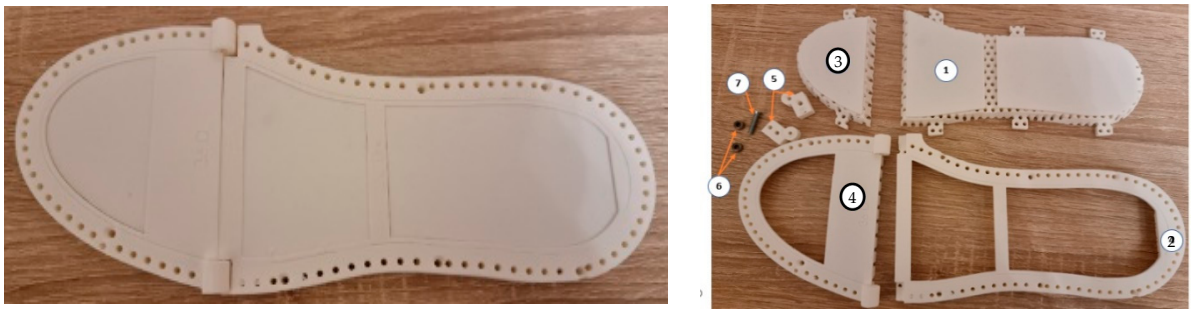
2.1.1. Mechanical Component

This part consists of two main parts (heel and tip parts), joined by a rotating joint (Figure 3). The tip and the heel have two subcomponents: the common element (Figure 3, elements 1 and 3) and the frame (Figures 3 and 4, elements 2 and 4).



a **b** **c**

Figure 3. Sandal sole—Solidworks design: (**a**) inside view of the sole; (**b**) exterior view sole; (**c**) the elements of the sole: 1—heel sole; 2—heel sole frame; 3—toe sole; 4—toe sole frame.



a **b**

Figure 4. Sandal sole—3D printer prototyping: (**a**) inside view of the sole; (**b**) the elements of the sole: 1—heel sole; 2—heel sole frame; 3—toe sole; 4—toe sole frame; 5, 6 and 7: rotating joint components: 5—bearing support, 6—bearing, 7—screw.

The pressure sensors are mounted on the back of the sole, which supports the foot. The pressure sensors can be mounted anywhere and in any configuration on the sole because it is perforated (on the back) with a matrix network of threaded holes in which the sensors are mounted.

The system is obtained by assembling these elements, depending on the requirements. First, sensory elements and common elements are used for all models (woman/man, sizes 36–41). Then, the frame type elements are changed depending on the characteristics, and the sensors are repositioned according to the predetermined model. Our research team manufactured all the components forming the system using a 3D printer and ABS filament

as raw material. The cost of a custom sandal sole, manufactured according to with user's particular specifications and needs, is around 5 Euro.

The components are assembled with screws. The fastening of the sandal straps is done on the sandal frame and allows any configuration of them due to a similar system with perforations. For different foot or lady/man sizes, change the frame, re-realizing the desired size of the shoes. This system is ergonomically minimizing the elements used. The straps have a VELCRO closure system, allowing a perfect fit.

2.1.2. Sensorial System

The sensory system comprises eight resistive pressure sensors mounted on the back of the sole. Sensors are positioned according to the pressure zones of the sole, having a proper positioning for each sandal size, made with a template. (Figure 5). The optimal positions were established by studying the existing insole models in trade, by studies performed on a group of people (male/female, different sizes) using pressure plates (for orthopaedical use), and by experimental positioning on the prototype obtained. As a result, an eight-sensor configuration was chosen to cover the sole's essential pressure areas.

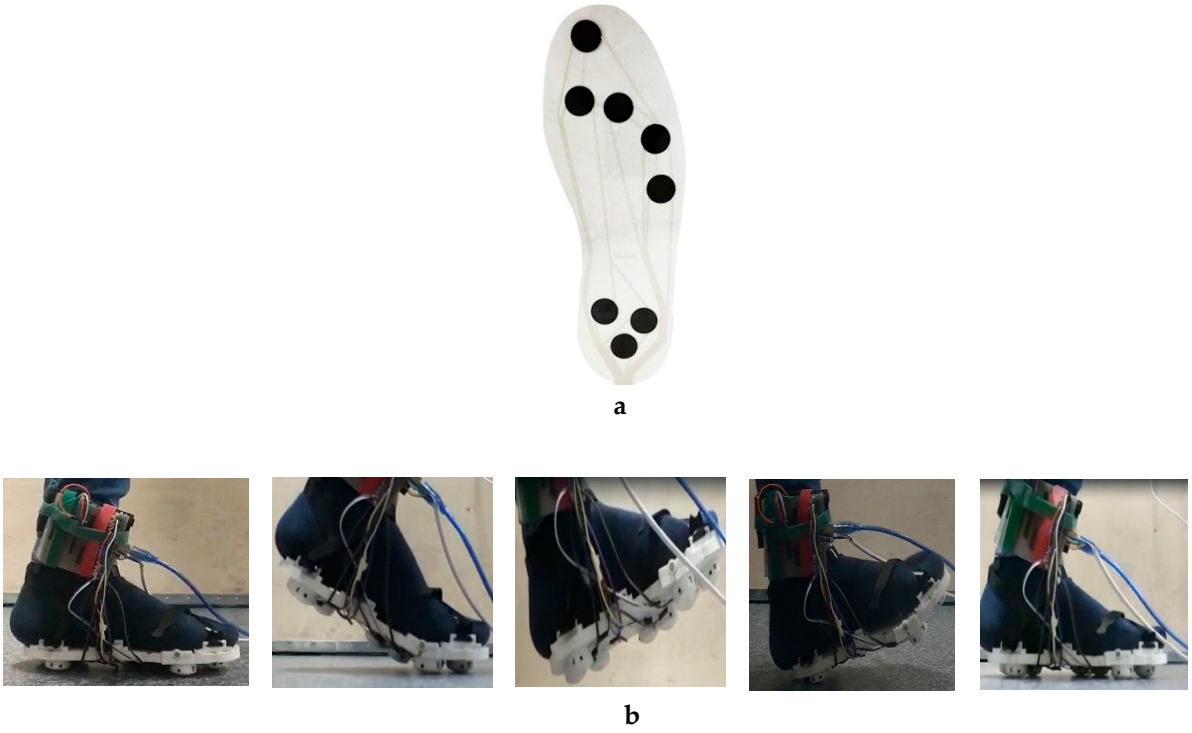


Figure 5. (**a**) Distribution of pressure sensors on the sole; (**b**) one-legged stepping cycle.

Each sensor is mounted in mechanical support fixed by a screw on the sandal's sole. This bracket consists of a cylindrical housing that supports the sensor. It is attached to the sole using an eccentric piece. When the sensor cannot be mounted precisely in the desired position, the eccentric part can reposition the cylindrical housing in the prescribed position. A sliding cylinder ending in a spherical cap represents the moving part and the contact with the ground. By pressing the sandal on the ground, this cap performs a translational movement in the cylindrical housing by pressing the pressure sensor. Thus the sensory network measures the distribution of body weight.

Figure 6 shows the conceptual photograph of the pressure sensor and an image of the sensor placed on the sole.

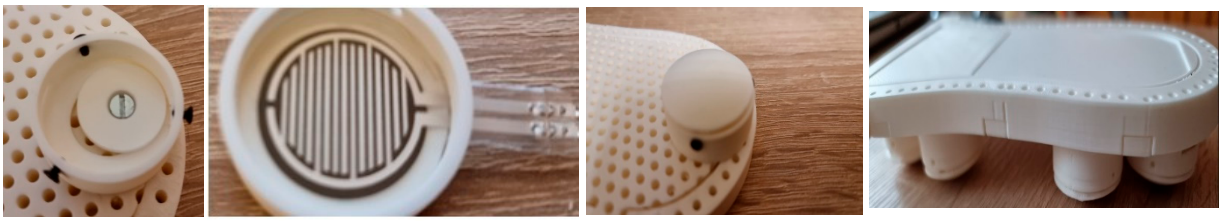
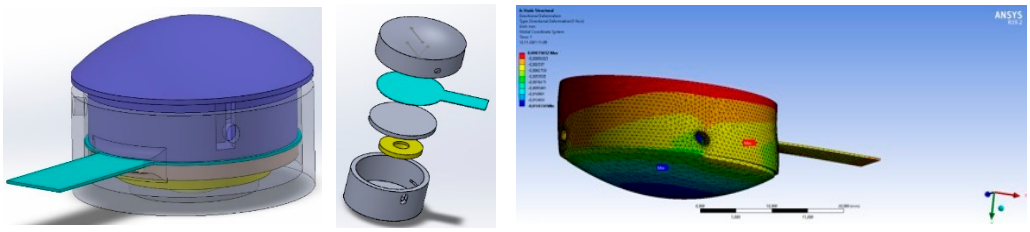


Figure 6. Sensor mounted on the sole of the sandal—prototype 3D printer, ABS—positioning detail using eccentric, sensor mounting detail in the housing.

All the components were designed using Solidworks and ANSYS, simulating accurate materials and stresses corresponding to the load with a body weight of 120 kg (Figure 7).



a **b**

Figure 7. (**a**) Sensor support components—Solidworks design—cylindrical housing, eccentric support mounting, sensor support base, pressure sensor, ground contact cylinder (finished with spherical part); (**b**) Sensor simulation details using ANSYS.

The aim is to use pressure (weight) sensors to determine the main points where the pressure exerted by each step is high. Given many sensors, an ATMEGA2560 controller was adopted because 8 sensors will be used for each sole, and the number of inputs held by the controller must be significant.

An FSR sensor is made of a piezoresistive material that can modify its resistance depending on the weight it measures. These sensors are resistors that vary linearly, considering conductance vs. resistance under an applied weight. The proposed application's advantages include the operation with low energy consumption and the fact that the implementation, as a thin film, allows mounting in very narrow and tight places.

The sensors are read using the electronic current-to-voltage converter circuit to obtain precise values of the measured weight. Such circuitry is required because the evolution of the signal provided by the sensor, depending on the weight, is recorded as current values (mA). The electronic circuit in Figure 8 takes the current as an input, providing a voltage value as output that can be read with the microcontroller. The MCP6004 operational amplifier is part of this design because it was necessary to obtain a linear signal compared to a classic voltage divider, and the current bias input is minimal. In addition, compared to a simple divider, this design keeps the same voltage applied to the FSR sensor even if other resistors or other sensors are connected in parallel.

The cost of the data acquisition system (sensors, circuits, processing unit) is around 200 Euro.

In addition, the theoretical principle of having a virtual ground between the terminals of the FSR sensor is applied. Finally, the formula determines the output voltage of the circuit:

$$V_{OUT} = \frac{-V_{DRIVE}}{R_{FSR}} \times R_F$$

where V_{OUT} represents the output voltage, $-V_{DRIVE}$ represents the supply voltage, and R_F is the load resistance.

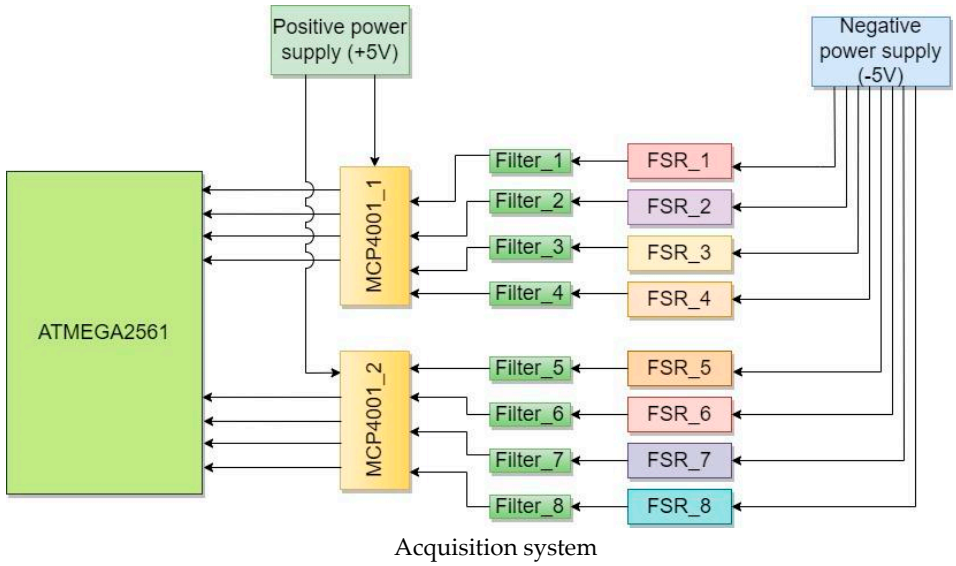


Figure 8. The hardware diagram.

It was decided to use the physical property. Namely, the conductance is obtained mathematically by the inverse of the resistance. The conductor's advantage is that the sensor has a linear evolution in weight detection based on this property. First, the conductor helps obtain the force, and then the force is transformed into mass.

2.2. Data Validation for the Sensorial System

Data validation is essential in any measurement process, mainly when the acquired data will be used as input for a control system—in our case, the gait control system for the lower limb prosthesis. We conducted a series of measurements to reveal the limits of the proposed sensorial systems under the terms of repeatability for each sensor, homogeneity among used sensors, and non-linearity. In this sense, the research team leased a calibration test weight kit, from an accredited metrological laboratory. The calibration test weight kit included several calibrated test weights, and the metrology laboratory presented the calibration certificate for them. The heaviest calibrated test weights included in the kit had the values of 1 kg, 5 kg and 10 kg, and they were used to test the repeatability of the sensorial element under various loads. The results obtained were correlated with determinations made with the pressure plate and were similar for several determinations.

2.2.1. General Testing Methodology

To obtain information as near as possible to the operation conditions, we conducted individual measurements for each of the eight sensorial element assemblies, (as shown in Figure 7, these are: the assembly formed by the cylindrical housing, eccentric support mounting, sensor support base, pressure sensor, and ground contact element). The methodology to record one set of data is:

- The team checks that the evaluated sensorial element's unique identifier is visible.
- The evaluated sensorial element is placed on a planar surface, with the cylindrical housing downwards and the ground contact element upwards.
- The evaluated sensorial element is electrically connected to the data acquisition system.
- All the electrical connections are verified visually for compliance with the wiring diagram.
- The calibrated test weights are placed for an easy and safe access.
- Preliminary readings are conducted to validate that the sensorial element, the data acquisition system and the data logging are working properly.
- The measurement protocol is conducted.
- The recorded data is verified for integrity.
- The recorded data is stored accordingly.

2.2.2. Repeatability Test Methodology

The repeatability test was designed to check the repeatability of the sensorial element, for three different calibrated test weights were used: 1 kg, 5 kg and 10 kg—thus also observing the (non)linearity. The measurement protocol for repeatability using a specific test weight is:

- The steps from the General methodology are conducted up until the conduction of the measurement protocol.
- On the measurement file, one research team member notes the evaluated sensorial element's unique identifier, the environmental conditions (temperature and humidity), and the value of the calibrated test weight used during the test.
- Another research team member places the calibrated test weight on the ground contact element of sensorial element (placed upwards, in this stage), assuring that the whole weight is supported only by the sensorial element.
- The weight is maintained on the sensorial element for 5 s.
- The research team member removes the weight from the sensorial element.
- The previous three steps are repeated ten times, respecting the repeatability conditions—within a short time interval and by the same research team member, without any recalibration or reinitialization of the data acquisition system. Each repetition is carried out as a standalone measurement—another research team member monitors the behaviour of the operator team member to be consistent and constant. The measurement is discarded if the monitoring team member observes deviations from those principles.

Following the data integrity check, the resulted dataset is subjected to validation and verification to find and eliminate possible random errors.

2.2.3. Dataset Processing for Repeatability

Since we expect to observe some oscillations of the values on the recorded datasets, we will determine the mean value for each repetition. In the computation of the mean value, we will consider only the values through stable measurements. Ten average values will be obtained for each repeatability dataset. Figure 9 shows an example of 5 recorded values. One can observe the loading phase of the sensorial element (noted with 1 on the figure), the stable measurement (noted 2) and the unloading stage (noted 3). The loading phase takes longer because the operator team member acts cautiously, not heavily, to hit the sensorial element. Unloading does not require such precautions.

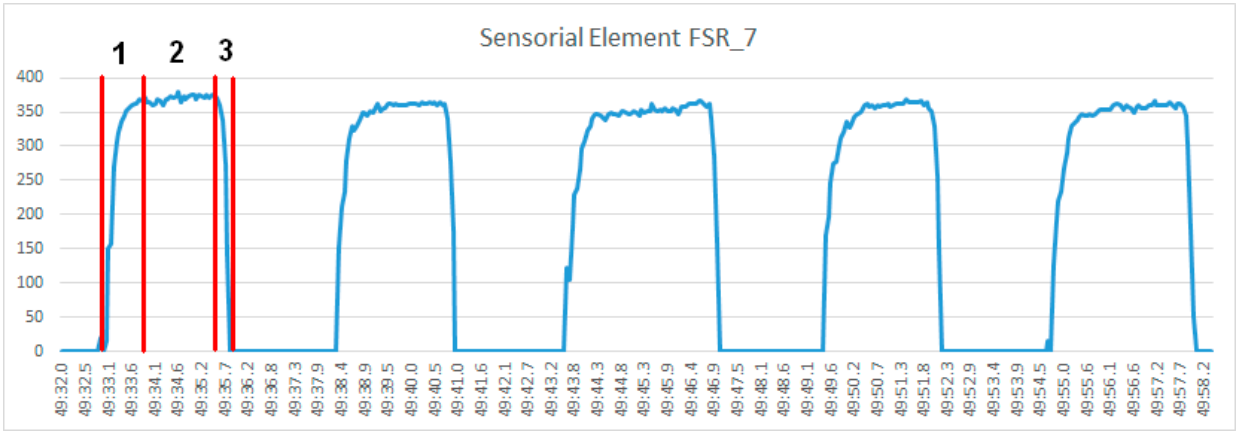


Figure 9. Sample from a repeatability dataset for FSR_7 sensor, using a 10 kg weight.

To conclude the sensorial element repeatability for a certain weight, we will compute the maximum recorded value, the minimum recorded value, the average and the standard deviation using the ten values, resulting in stable measurements. For example, suppose one sensorial element will exhibit a standard deviation higher than 10% of the mean value

for any three recorded datasets (1 kg, 5 kg, 10 kg). In that case, the sensor will be rejected and replaced.

2.2.4. Homogeneity Test Measurement

After determining the repeatability of each sensor, which guarantees its stable behaviour, the research team will compare the results obtained for each sensorial element. If there will be differences among the mean values provided by different sensorial elements for the same loading weight, then we will determine the highest mean value among the eight sensorial elements.

For each of the other sensing elements, a gain factor will be determined as a proportional ratio between the highest determined mean value and the mean value for the current sensorial element.

The computed gain factor will be applied for all the future measurements.

Thus, all the sensorial element outputs will be normalized concerning the most responsive sensor.

2.3. Methodology for Measuring the Gait of Healthy Persons

The proposed lower limb prosthesis, on the one hand, will reproduce the gait of the person using it. On the other hand, it will be adapted and synchronized to the instantaneous gait of the person using it. To develop proper control algorithms for the lower limb prosthesis is necessary first to observe the gait of a regular person. To conduct those measurements, the following data recording methodology was established:

- The steps from the general methodology are completed up until the conduction of the measurement protocol.
- The measurement protocol is presented and explained to the subject.
- The subject is shod with the sandal soles.
- One research team member notes the subject's assigned ID (see Section 2.4).
- The subject is asked to walk several steps, gaiting as naturally as he can.
- The resulted dataset is subjected to a process of validation and verification to find and eliminate possible random errors.

2.4. Ethical Considerations

Since the measurements which will be presented in this paper involved human subjects, the proposed methodologies were designed, and the measures were conducted considering the applicable statements from the Ethical Principles for Medical Research Involving Human Subjects—Declaration of Helsinki developed by The World Medical Association (WMA), and all the applicable national legislation–Law 95/2006 regarding the health care system reform, Law 43/2003 regarding the patient rights, Ministry of Health Order No. 1502/2016, national guidelines for ethical principles in medical research on human subjects. Before conducting the measurements, the human subjects were informed about the purpose of the measurements, the goals it proposes, the expected duration for one measurement set, the procedures that will take place, the known risks and the possible inconveniences that it may cause, the payable benefits, the anonymization procedure of the data gathered during the measurements, how the recorded data it may be used it for research activities and the scientific research publication of the research results. All the human subjects were informed, and they understood and accepted that participation was voluntary, without being paid. Consent forms were presented to the participants, containing all the information described above. The research team ensured that the participants understood all the above information before signing the consent forms. Because the sensory system was designed to be worn over ordinary shoes and clothing without the need for medical drugs or invasive physical items, no requirements from the Ethics Commission for research involving human subjects were violated. Data anonymization is done using an alphanumeric code (ID) for each subject's dataset.

3. Results

Based on the methodologies presented in Section 2.3, the research team conducted the according to measurements. The obtained results are presented as follows.

3.1. Repeatability Measurements

All the sensorial elements were tested according to the methodology presented in Section 2.2.2 for repeatability. The research team conducted three repeatability tests—one repeatability test for each of the test weights—1 kg, 5 kg and 10 kg, and in the first stage, eight different sensorial elements were tested. The results are presented in Table 1.

Table 1. Repeatability test results.

Test Weight	Sensorial Element ID	Value 1	Value 2	Value 3	Value 4	Value 5	Value 6	Value 7	Value 8	Value 9	Value 10	Avg	SD (%)
1 kg	FSR_0	110	140	141	132	108	103	106	138	124	116	121.8	12.39
	FSR_1	119	118	96	121	73	64	100	59	110	84	94.4	24.46
	FSR_2	41	53	74	90	63	76	49	59	63	70	63.8	21.94
	FSR_3	102	90	99	101	98	99	108	94	102	91	98.4	5.56
	FSR_4	38	37	26	30	38	31	34	37	31	32	33.4	11.97
	FSR_5	45	52	43	57	37	52	50	52	44	48	48	12.10
	FSR_6	74	66	79	56	63	64	82	55	82	73	69.4	14.40
	FSR_7	102	67	98	97	73	50	79	68	65	51	75	25.40
5 kg	FSR_0	154	170	174	187	190	157	188	167	144	146	167	10.17
	FSR_1	204	186	157	147	165	197	189	199	193	228	186.5	12.93
	FSR_2	211	201	197	217	228	222	221	214	234	207	215.2	5.40
	FSR_3	200	210	204	196	201	181	198	197	214	193	199.4	4.56
	FSR_4	180	189	192	170	187	190	172	191	183	187	184.1	4.23
	FSR_5	55	60	52	72	60	60	68	56	61	61	60.5	9.73
	FSR_6	213	192	186	194	191	194	216	220	192	217	201.5	6.55
	FSR_7	214	222	227	219	207	220	196	222	212	211	215	4.20
10 kg	FSR_0	308	271	283	277	295	295	315	307	294	264	292	5.60
	FSR_1	287	248	368	317	366	437	345	351	345	270	331.2	15.91
	FSR_2	202	209	215	202	204	210	210	209	230	211	209.8	3.71
	FSR_3	275	336	260	267	284	279	322	316	340	293	298.5	9.36
	FSR_4	267	226	239	232	223	229	217	222	221	226	230.1	5.91
	FSR_5	144	136	114	147	175	105	116	102	101	100	123.6	19.51
	FSR_6	185	187	202	209	215	211	216	224	253	290	219.2	13.60
	FSR_7	325	316	317	323	310	311	312	311	294	304	312	2.73

The maximum load of the sensors used in the sensorial element is, according to their datasheet, 50 kg. The datasets were recorded as digital values, where 0 represents the absence of the weight load on the sensor, and the maximum digital value is 1024. Value 1 to Value 10 represents the mean value recorded during the stable measurement phase, presented in Section 2.2.2, Figure 10. Therefore, we considered it more beneficial to indicate the standard deviation as a percentage related to its average value computed over the ten measurements, under the SD (%) column.

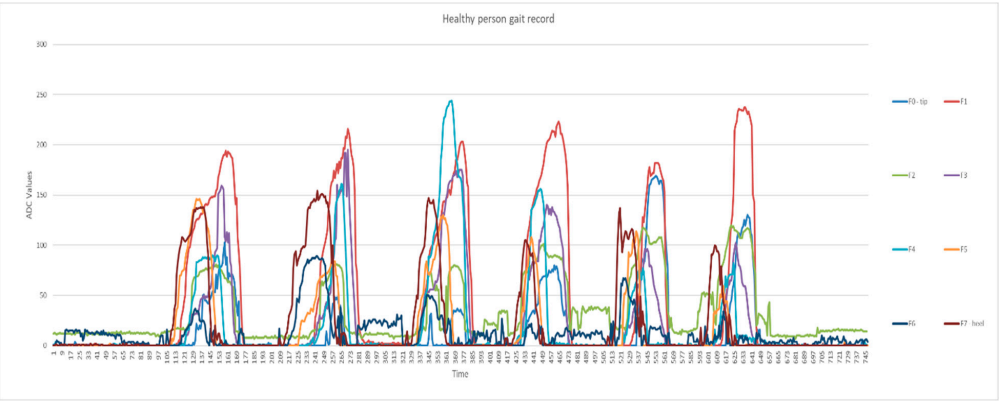


Figure 10. The gait record for a healthy person's left leg.

We analyzed the data from Table 1 following the criteria enounced in Section 2.2.2, especially the data obtained for measurements conducted for the 10 kg test weights. We noted that the FSR_1, FSR_5 and FSR_6 exhibit a standard deviation (SD%) higher than 10% of the mean value. Therefore, we concluded that the sensors used on the sensorial elements cannot provide reliable, repeatable data. Based on this analysis, the research team decided to replace them with similar sensors, which passed a similar repeatability test. Another conclusion regards the readings for the 1 kg load. Since the maximum load for a sensor is 50 kg, and 1 kg represents 2% of its full load, one can observe that the standard deviation exhibits high percentage values; thus, the repeatability is low. However, since such low loads appear only in short, transitory moments between gait phases, we can consider them acceptable.

Also, one can note that the output response of the sensors is powerful nonlinear. Thus, in future work, we will consider using more test weight values to determine the nonlinear characteristic.

3.2. Homogeneity Results

Another finding after concluding the repeatability tests is that the sensors' output response isn't homogenous—different sensorial elements offer different output values for the same load—still providing good repeatability for that output. Thus, the research team determined a proportional ratio between the highest value offered by one of the sensorial elements FSR_0 . . . FSR_7 and the value for a specific sensorial element. Finally, the computed gain factors are applied for all the following presented measurements.

3.3. Records of the Gait of Healthy Persons

After the data validation for the sensorial system was concluded, the research team recorded the gait of healthy persons according to the methodology described in Section 2.4. The records were conducted for 10 healthy persons, chosen among the projects research team members We were looking to have representatives of both genders, covering as wide a range of age, weight and footwear size as possible. The measurements were conducted for 4 females and 6 males. We tested EU footwear sizes of 35, 36, 37 (for females) and 41, 42, 43 and 44 (for males). The body weight varied between 46 to 57 kg (for females) and 70 to 85 kg (for males). The height varied between 1.65m to 1.75m (for females) and 1.71 to 1.84 (for males). All the ten participants were evaluated, from an orthopedic point of view, by the specialist doctor also member the project—none exhibited orthopedic defficiencies. Also, their gait was evaluated.

Then, we analyzed the pressure distribution evolution over time, as revealed by the sensorial elements mounted on the sandal soles—Figure 11. Figure 11 represents the weight distribution on the sole, in the stepping cycle, for one foot: 1—foot in balance-contact with the heel, 2—contact with the heel plus the middle part of the sole, 3-4-5—firm contact with the sole, support on one foot, the other foot in the balance, 6—lifting the heel off the ground, 7—support only on the front of the sole, 8—support on the toe (toes), lifting the foot off the ground and entering the balance.

Each of the individual sensorial elements can sustain a load of up to 50 kg. The dataset illustrated in Figure 11. is recorded for a person weighing approx. 60 kg. Thus, the loading on each sensor does not reach high values, as one can observe.

The recorded data, displayed in Figures 10 and 11, are consistent with the plantar pressure measurements recorded using other traditional plantar measurement devices [11,41].

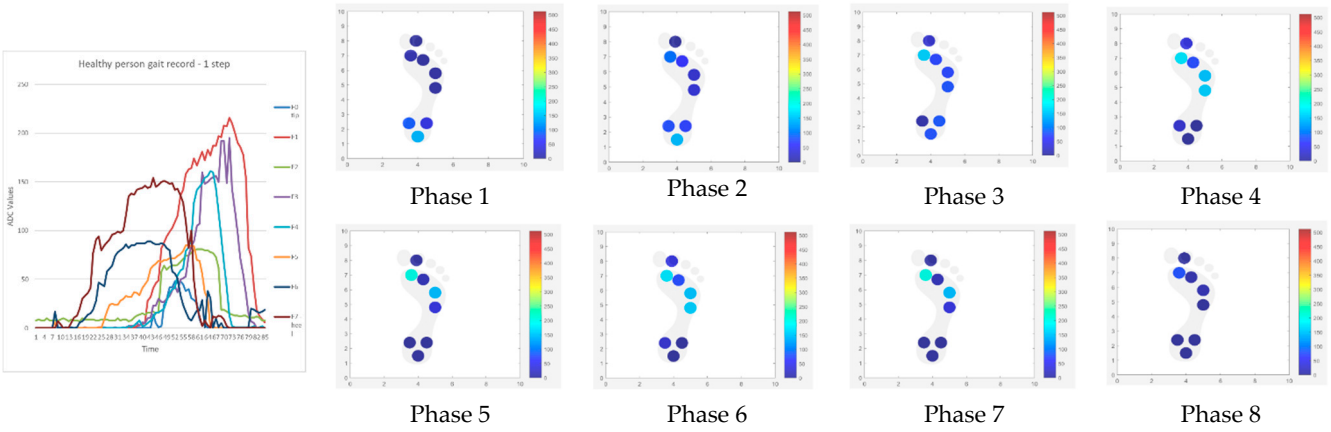


Figure 11. The eight-step phases are recorded data for one step, healthy person gait, right foot, and loading on the sensorial elements.

4. Discussion

The design and development of functional prostheses with limited capabilities (passive or quasi-passive protections) were considered. Then prostheses with more advanced features (semi-active or active) appeared, allowing the control of gait adaptable to different types of terrain with minimal difficulty.

There are several theoretical models proposed to be applied to the ankle-foot prosthesis. For example, a quasi-passive ankle prosthesis was designed by Collins and Kuo [42]. This prosthesis recycles energy when touched with the heel and returns it to the user in the terminal phase of the step. Another example of a prosthetic foot was developed by Grabowski et al. [43]. Although it had some durability limitations, this prosthesis could emulate the torques produced by the human ankle through cables, urethane springs, and fiberglass elements. However, it also had some durability limitations. Finally, Hansen and Nickel [44] proposed a passive ankle-foot prosthesis that operated in two states: standing and walking, by incorporating a locking mechanism to separate these phases.

Subsequently, the main challenge in developing ankle-foot prostheses was implementing active protections. In addition, these prostheses require considerable power and precise control of the impedance torque. Hitt et al. [45] presented a model of the robotic transtibial prosthesis called SPARKY to reduce the power demand. They used biomechanical energy regeneration technology to reduce energy consumption by combining spring and a mechanical tendon actuator. In 2012, Herr and Grabowski presented an ankle-foot prosthesis that closely mimicked the function of the human ankle and provided a net-positive power while walking. It is powered by a 200 W brushless DC motor and a series ball screw with a carbon composite lamellar spring [46]. Bergelin and Voglewede propose an active prosthesis using a four-bar mechanism and offering a range of motion similar to that of the human ankle, according to the results obtained from the simulations [47]. Finally, Cherelle et al. have a prosthesis that stores energy in the springs during the complete position phase, then released on push, and can provide all the power needed for forwarding propulsion with a low-power actuator [48].

There is currently a wide range of smart foot prostheses in which various sensors and electromechanical devices are installed to reproduce a more biological aspect of the human foot. In the case of prostheses, we should have a smart sole installed on the prosthetic foot so that it accurately captures real-time contact information through plantar pressure measurements. There are a variety of plantar pressure measuring systems, which can generally be classified into platform systems and shoe systems.

The advantages and limitations of foot pressure equipment were some of the health concerns of the subjects tested. The number of sensors for sufficient coverage of the foot regions is the fundamental condition to opt either for the plantar platform or the footwear system. In addition, a higher frequency sampling rate of the system can provide more

accurate results. Variations in the morphology of the human foot depending on sex, age, and body mass must also be considered. Problems with foot pressure sensitivity, external load impact, and duration may occur during practical training. In most cases, qualitative data must be systematically collected through an appropriate experimental design when subjects perform a normal gait, considering those control variables, such as standard gait time (gait cycle) and cadence. Potential future directions of exploration would include different types of surface roughness to varying angles of inclination that affect the level of sensitivity to foot pressure.

Among the systems for measuring plantar pressure for gait analysis, the plantar insoles are widely used and cause many locomotion disorders. Although the soles of the feet provide information only in the positional phase, they are sufficient for most gait rehabilitation systems, posture control and balance [41]. For example, Razak et al. [49] specified in their study that the location of the sensors was determined, taking into account only the dominant pressure points of the plantar surface during walking. Most insoles obtain the necessary information from a discrete number of sensors (the minimum number varies from 2 to 16 or more, depending on the need).

5. Conclusions

This work presented a novel low-cost lower limb prosthesis based on sensors placed in a plantar insole. The proposed platform has the following advantages:

- It can be used for any type or size of foot.
- It is designed modularly, allowing most components to be reused when reconfiguring for another foot size.
- The soleplate allows you to reconfigure the number of sensors and their positioning.
- The sole allows you to adjust the position of the straps on the sandals.
- Clamping systems (sandals and gyroscopic sensors) allow an optimal adjustment.
- The system can be extended in terms of pressure and gyroscopic sensors.
- The purchasing system is light and similar to a regular pair of shoes, limiting errors as it does not disturb the gait.
- Data acquisition accuracy far exceeds the needs of such a system.
- The simplified and optimized system can be integrated into a prosthesis, constantly coordinating its configuration depending on the step phase and the type of movement.
- The cost of the data acquisition system is around 200 Euro, which can thus be considered low cost and high-efficiency.

6. Patents

Patent application—A/00213/2019: Spherical joint based on intelligent fluids [39].

Author Contributions: Conceptualization, C.F.P., L.F.M. and I.C.V.; methodology, L.F.M.; validation, L.F.M., I.C.V. and Ș.I.C.; formal analysis, C.F.P., L.F.M. and I.C.V.; investigation, C.F.P., L.F.M., I.C.V. and D.C.; resources, C.F.P., F.L.P. and Ș.I.C.; data curation, C.F.P., L.F.M., Ș.I.C. and F.L.P.; writing—original draft preparation, C.F.P., L.F.M. and I.C.V.; writing—review and editing, C.F.P., L.F.M. and I.C.V.; supervision, C.F.P., L.F.M., I.C.V., D.C. and N.B.; project administration, C.F.P., L.F.M. and I.C.V.; funding acquisition, N.B. All authors have read and agreed to the published version of the manuscript.

Funding: This research was funded by PNIII scheme, Program 2: Increasing the competitiveness of the Romanian economy through RDI, Subprogram 2.1: Competitiveness through research, development and innovation—Experimental project—demonstration, grant number 344PED/2020 and POC-Competitiveness Operational Program.

Institutional Review Board Statement: The study was conducted according to the guidelines of the Declaration of Helsinki. Ethical review and approval were waived for this study due to all the measurements being performed using non-invasive, contactless devices and no administration of medical drugs were required in the process. To assure that all the ethical principles were respected during our research work, we contracted an external consultant, RehabMed, which assisted us during all the research phases.

Informed Consent Statement: Informed consent was obtained from all subjects involved in the study.

Data Availability Statement: Not applicable.

Acknowledgments: This work was supported by a grant of the Romanian Ministry of Education and Research, CCCDI—UEFISCDI, project number PN-III-P2-2.1-PED-2019-0937, within PNCDI III;HUB-UCv-Support Center for International RD Projects for the Oltenia region-cod SMIS 107885.

Conflicts of Interest: The authors declare no conflict of interest.

References

1. McDonald, C.L.; Westcott-McCoy, S.; Weaver, M.R.; Haagsma, J.; Kartin, D. Global prevalence of traumatic non-fatal limb amputation. *Prosthet. Orthot. Int.* **2021**, *45*, 105–114. [CrossRef] [PubMed]
2. Hughes, W.; Goodall, R.; Salciccioli, J.D.; Marshall, D.C.; Davies, A.H.; Shalhoub, J. Trends in Lower Extremity Amputation Incidence in European Union 15+ Countries 1990–2017, Editor's Choice. *Eur. J. Vasc. Endovasc. Surg.* **2020**, *60*, 602–612. [CrossRef] [PubMed]
3. Walter, N.; Alt, V.; Rupp, M. Lower Limb Amputation Rates in Germany. *Medicina* **2022**, *58*, 101. [CrossRef] [PubMed]
4. Laferrier, J.Z.; Groff, A.; Hale, S.; Sprunger, N.A. A Review of Commonly Used Prosthetic Feet for Developing Countries: A Call for Research and Development. *J. Nov. Physiother.* **2018**, *8*, 380. [CrossRef]
5. Versluys, R.; Beyl, P.; van Damme, M.; Desomer, A.; van Ham, R.; Lefeber, D. Prosthetic feet: State-of-the-art review and the importance of mimicking human ankle-foot biomechanics. *Disabil. Rehabil. Assist. Technol.* **2009**, *4*, 65–75. [CrossRef]
6. Voloshina, A.S.; Collins, S. A Review of Design and Control Approaches in Lower-Limb Prosthetic Devices. *Biology* **2019**. Available online: https://www.semanticscholar.org/paper/A-Review-of-Design-and-Control-Approaches-in-Voloshina-Collins/90dc85af676c1c01301d941a2d0b8de4e1d9c9a1 (accessed on 8 January 2022).
7. Schmalz, T.; Blumentritt, S.; Jarasch, R. Energy expenditure and biomechanical characteristics of lower limb amputee gait: The influence of prosthetic alignment and different prosthetic components. *Gait Posture* **2002**, *16*, 255–263. [CrossRef]
8. Mattes, S.; Martin, P.; Royer, T. Walking symmetry and energy cost in persons with unilateral transtibial amputations: Matching prosthetic and intact limb inertial properties. *Arch. Phys. Med.* **2000**, *81*, 561–568. [CrossRef]
9. Tesio, L.; Lanzi, D.; Detrembleur, C. The 3-D motion of the centre of gravity of the human body during level walking. II. Lower limb amputees. *Clin. Biomech.* **1998**, *13*, 83–90. [CrossRef]
10. Klute, G.K.; Czernieki, J.; Hannaford, B. Development of powered prosthetic lower limb. In Proceedings of the 1st Natl Meeting, Veterans Affairs Rehabil. R&D Service, Washington, DC, USA, 1–3 October 1998.
11. Chen, L.; Wang, C.; Wang, J.; Song, X. Design of Hybrid Phase Sliding Mode Control Scheme for Lower Extremity Exoskeleton. *Appl. Sci.* **2019**, *9*, 3754. [CrossRef]
12. Vickers, D.R.; Palk, C.; McIntosh, A.S.; Beatty, K.T. Elderly uni-lateral transtibial amputee gait on an inclined walkway: A biomechanical analysis. *Gait Posture* **2008**, *27*, 518–529. [CrossRef] [PubMed]
13. Torburn, L.; Schweiger, G.P.; Perry, J.; Powers, C.M. Below-knee amputee gait in stair ambulation. *Clin. Orthop. Relat. Res.* **1994**, *303*, 185–192. [CrossRef]
14. Au, S.K.; Bonato, P.; Herr, H. An EMG-position controlled system for an active ankle-foot prosthesis: An initial experimental study. In Proceedings of the 9th International Conference on Rehabilitation Robotics, Chicago, IL, USA, 28 June–1 July 2005; pp. 375–379. [CrossRef]
15. Au, S.K.; Herr, H. Initial experimental study on dynamic interaction between an amputee and a powered ankle-foot prosthesis. In Proceedings of the Workshop on Dynamic Walking: Mechanics and Control of Human and Robot Locomotion, Ann Arbor, MI, USA, 6–8 May 2006.
16. Hitt, J.; Bellman, R.; Holgate, M.; Sugar, T.; Hollander, K. The sparky (spring ankle with regenerative kinetics) projects: Design and analysis of a robotic transtibial prosthesis with regenerative kinetics. In Proceedings of the ASME International Design Engineering Technical Conferences and Computers and Information in Engineering Conference, DETC2007, Las Vegas, NV, USA, 4–7 September 2007; pp. 1587–1598.
17. Au, S.K.; Herr, H.M. Powered ankle-foot prosthesis: The importance of series and parallel motor elasticity. *IEEE Robot. Autom. Mag.* **2008**, *15*, 52–59. [CrossRef]
18. Zhao, S.; Lei, Y.; Wang, Z.; Zhang, J.; Liu, J.; Zheng, P.; Gong, Z.; Sun, Y. Biomimetic Artificial Joints Based on Multi-Material Pneumatic Actuators Developed for Soft Robotic Finger Application. *Micromachines* **2021**, *12*, 1593. [CrossRef] [PubMed]
19. Tabucol, J.; Brugo, T.M.; Povolo, M.; Leopaldi, M.; Oddsson, M.; Carloni, R.; Zucchelli, A. Structural FEA-Based Design and Functionality Verification Methodology of Energy-Storing-and-Releasing Prosthetic Feet. *Appl. Sci.* **2022**, *12*, 97. [CrossRef]

20. Russo, M.; Chaparro-Rico, B.D.M.; Pavone, L.; Pasqua, G.; Cafolla, D. A Bioinspired Humanoid Foot Mechanism. *Appl. Sci.* **2021**, *11*, 1686. [CrossRef]
21. Fridman, A.; Ona, I.; Isakov, E. The influence of prosthetic foot alignment on trans-tibial amputee gait. *Prosthet. Orthot. Int.* **2003**, *27*, 17–22. [CrossRef]
22. Lemaire, E.D.; Samadi, R.; Goudreau, L.; Kofman, J. Mechanical and biomechanical analysis of a linear piston design for angular-velocity-based orthotic control. *J. Rehabil. Res. Dev.* **2013**, *50*, 43–52. [CrossRef]
23. Sewell, P.; Noroozi, S.; Vinney, J.; Andrews, S. Developments in the trans-tibial prosthetic socket fitting process: A review of past and present research. *Prosthet. Orthot. Int.* **2000**, *24*, 97–107. [CrossRef]
24. Hernández-Acosta, M.A.; Torres-San Miguel, C.R.; Piña-Díaz, A.J.; Paredes-Rojas, J.C.; Aguilar-Peréz, L.A.; Urriolagoitia-Sosa, G. Numerical Study of a Customized Transtibial Prosthesis Based on an Analytical Design under a Flex-Foot® Variflex® Architecture. *Appl. Sci.* **2020**, *10*, 4275. [CrossRef]
25. Faragó, P.; Grama, L.; Farago, M.-A.; Hintea, S. A Novel Wearable Foot and Ankle Monitoring System for the Assessment of Gait Biomechanics. *Appl. Sci.* **2021**, *11*, 268. [CrossRef]
26. Amaro, C.M.; Castro, M.A.; Roseiro, L.; Neto, M.A.; Amaro, A.M. Plantar Pressure Evaluation during the Season in Five Basketball Movements. *Appl. Sci.* **2020**, *10*, 8691. [CrossRef]
27. Deffenbaugh, B.W.; Herr, H.; Pratt, G.A.; Wittig, M.B. Electronically Controlled Prosthetic Knee. U.S. Patent WO2001054630A1, 2 August 2001. Available online: https://patents.google.com/patent/WO2001054630A1 (accessed on 12 January 2022).
28. Available online: https://www.ossur.com/en-gb (accessed on 12 January 2022).
29. Herr, H.; Wilkenfeld, A. User-adaptive control of a magnetorheological prosthetic knee. *Ind. Robot Int. J.* **2003**, *30*, 42–55. [CrossRef]
30. Thorarinsson, E.T.; Jonsdottir, F.; Palsson, H. Design of a Magnetorheological Prosthetic Knee. In Proceedings of the NordDesign 2006, Reykjavik, Iceland, 16–18 August 2006. Available online: https://www.semanticscholar.org/paper/Design-of-a-Magnetorheological-Prosthetic-Knee-Thorarinsson-Jonsdottir/2fb5d016910572203a45070b04e308c8033df2d1 (accessed on 12 January 2022).
31. Herr, H.M.; Weber, J.A.; Casler, R.J., Jr. Biomimetic Joint Actuators. U.S. Patent WO2012125562A1, 20 September 2012. Available online: https://patents.google.com/patent/WO2012125562A1/en (accessed on 12 January 2022).
32. de Andrade, R.M.; Martins, J.S.R.; Pinotti, M.; Filho, A.B.; Vimieiro, C.B.S. Novel active magnetorheological knee prosthesis presents low energy consumption during ground walking. *J. Intell. Mater. Syst. Struct.* **2021**, *32*, 1591–1603. [CrossRef]
33. Narang, Y.S.; Arelekatti, V.N.; Winter, A.G. The Effects of Prosthesis Inertial Properties on Prosthetic Knee Moment and Hip Energetics Required to Achieve Able-Bodied Kinematics. *IEEE Trans. Neural Syst. Rehabil. Eng.* **2016**, *24*, 754–763. [CrossRef]
34. Murthy Arelekatti, V.N.; Winter, A.G. Design and Preliminary Field Validation of a Fully Passive Prosthetic Knee Mechanism for Users with Transfemoral Amputation in India. *ASME J. Mech. Robot.* **2018**, *10*, 031007. [CrossRef]
35. Pinto Maquilon, J.K.; Velasquez, M.C. Durability of lower limb prostheses with low-cost exoskeletal technology, in patients with lower limb amputatispeta to any cause. *Ann. Phys. Rehabil. Med.* **2018**, *61*, e470–e471. [CrossRef]
36. Vladu, I.C.; Pană, C.F.; Copiluși, C.; Petrișor, I.; Vladu, I.; Bîzdoacă, N.G. *Controllable Passive Transtibial Prosthesis—Design, Book Mechanisms and Machine Science, Advances in Service and Industrial Robotics, Mechanisms and Machine Science*; Springer: Berlin/Heidelberg, Germany, 2021; Volume 102, pp. 176–183, ISSN1 2211-0984/ISSN2 2211-0992 (electronic). ISBN1 978-3-030-75258-3/ISBN2 978-3-030-75259-0 (eBook), 9-0 (eBook).
37. Powered Lower-Limb Prostheses. Available online: http://research.vuse.vanderbilt.edu/cim/research_leg.html (accessed on 10 January 2022).
38. Willick, S.E. The athlete with limb deficiency, Paralympic Athletes Targeted Topic, ASPETAR. Sports Medicine Journal. Available online: https://www.aspetar.com/journal/viewarticle.aspx?id=432#.Ynx8TuhBxPY (accessed on 10 January 2022).
39. Cristian, I.V.; Cristina, F.P.; Viorel, S.; Daniela, M.P.-P.; Ileana, V.; Dan Cristian, G.; Daniela, T.; Nicu, G.B. Spherical Joint Based on Intelligent Fluids. Patent Application A/00213/2019, 4 May 2019.
40. Lorkowski, J.; Gawronska, K.; Pokorski, M. Pedobarography: A Review on Methods and Practical Use in Foot Disorders. *Appl. Sci.* **2021**, *11*, 11020. [CrossRef]
41. Wafai, L.; Zayegh, A.; Woulfe, J.; Aziz, S.M.; Begg, R. Identification of Foot Pathologies Based on Plantar Pressure Asymmetry. *Sensors* **2015**, *15*, 20392–20408. [CrossRef]
42. Collins, S.H.; Ku, A.D. Recycling energy to restore impaired ankle function during human walking. *PLoS ONE* **2010**, *5*, e9307. [CrossRef]
43. Grabowski, A.M.; Rifkin, J.; Kra, R. K3 promoter prosthetic foot reduces the metabolic cost of walking for unilateral transtibial amputees. *J. Prosthet. Orthot.* **2010**, *22*, 113–120. [CrossRef]
44. Hansen, A.H.; Nicke, E.A. Development of a bimodal ankle-foot prosthesis for walking and standing/swaying. *J. Med. Devices* **2013**, *7*, 035001. [CrossRef]
45. Hitt, J.K.; Sugar, T.G.; Holgate, M. An active foot-ankle prosthesis with biomechanical energy regeneration. *J. Med. Devices* **2010**, *4*, 011003. [CrossRef]
46. Herr, H.M.; Grabowski, A.M. Bionic ankle–foot prosthesis normalizes walking gait for persons with leg amputation. *Proc. R. Soc. Lond. B Biol. Sci.* **2012**, *279*, 457–464. [CrossRef]

47. Bergelin, B.J.; Voglewede, P.A. Design of an active ankle-foot prosthesis utilizing a four-bar mechanism. *J. Mech. Des.* **2012**, *134*, 061004. [CrossRef]
48. Cherelle, P.; Grosu, V.; Matthys, A. Design and validation of the ankle mimicking prosthetic (AMP-) foot 2.0. *IEEE Trans. Neural Syst. Rehabilit. Eng.* **2014**, *22*, 138–148. [CrossRef]
49. Abdul Razak, A.H.; Zayegh, A.; Begg, R.K.; Wahab, Y. Foot plantar pressure measurement system: A review. *Sensors* **2012**, *12*, 9884–9912. [CrossRef]